A highly sensitive octopus-like azobenzene fluorescent probe for determination of abamectin B_1 in apples

Zhenlong Guo
Beijing Forestry University
YiFei Su
Beijing Forestry University
Kexin Li
Beijing Forestry University
MengYi Tang
Beijing Forestry University
Qiang Li (liqiang@bjfu.edu.cn)
Beijing Forestry University
Shandong Xu
Beijing Forestry University

Research Article

Keywords: azobenzene fluorescent probe, abamectin B1

Posted Date: November 20th, 2020

DOI: https://doi.org/10.21203/rs.3.rs-109482/v1

Version of Record: A version of this preprint was published at Scientific Reports on February 25th, 2021.
See the published version at https://doi.org/10.1038/s41598-021-84221-w.

Abstract

The development of detecting residual level of abamectin B1 in apples is of great importance to public health. Herein, we synthesized a octopus-like azobenzene fluorescent probe 1,3,5-tris (5'-[(E)-(p-phenoxyazo) diazenyl)] benzene-1,3-dicarboxylic acid) benzene (TPB) for preliminary detection of abamectin B1 in apples. The TPB molecule was characterized by ultraviolet-visible absorption spectrometry, 1H-nuclear magnetic resonance, fourier-transform infrared (FT-IR), electrospray ionization mass spectroscopy (ESI-MS) and fluorescent spectrum. A proper determination condition was optimized, with limit of detection and limit of quantification of 1.3 μg L-1 and 4.4 μg L-1, respectively. The mechanism of this probe to identify abamectin B1 was illustrated in terms of undergoing aromatic nucleophilic substitution, by comparing fluorescence changes, FT-IR and ESI-MS. Furthermore, a facile quantitative detection of the residual abamectin B1 in apples was achieved. Good reproducibility was shown based on relative standard deviation of 2.20%. Six carboxyl recognition sites, three azo groups and unique fluorescence signal towards abamectin B1 of this fluorescent probe decided ideal sensitivity, specificity and selectivity. The results show that the octopus-like azobenzene fluorescent probe may be promising for evaluating abamectin B1 in agricultural foods.

Introduction

Avermectins, being one type of macrolide antibiotics, have been widely used as bactericide, insecticide and miticide for plants or animals, and have excellent characteristics of disturbing the target's neurophysiological activities and can easily be decomposed by soil microorganisms[1]. Abamectin B_1, is the only avermectin that is widely approved for plants and animals for its efficient antiparasitic activity[2,3]. However, wide use of avermectins usually leads to consecutive accumulation in food-producing animals and plants[4,5]. To detect avermectins (Abamectin B_1), various analytical approaches were used. The approaches include high-performance liquid chromatography-ultraviolet detection (HPLC-UV)[4], liquid chromatography-tandem mass spectrometry (LC-MS)[6], high-performance liquid chromatography-fluorescent detector (HPLC-FLD)[7], enzyme-linked immunosorbent assay (ELISA)[8] and liquid chromatography-tandem mass spectrometry/mass spectrometry (HPLC-MS/MS)[9]. However, these approaches either needed a time-consuming process, high-cost accurate instrument, or high professional operators, which makes them difficult to apply in general laboratories[10]. Herein, considering the potential harm of abamectin B_1 for public health, a convenient and accurate analysis method for residual abamectin B_1 is necessary[10,11]. Therefore, it is necessary to explore a convenient analysis method for detection of residual abamectin B_1 to reduce the potential harm to public health.

Ultilization of fluorescent probe has gained great attention in recent years owing to the advantages of high sensitivity, high selectivity, fast response, low cost, and direct detection[12]. Especially, azobenzene fluorescent probe exhibits outstanding fluorescent quantum yield, light stability[13], and good chemical and thermal stability[14]. Fluorescent probe has been applied to analyse organophosphorus pesticides[15],

organochlorine pesticides[16] and carbamate pesticides[17]. However, few studies on fluorescent probe for monitoring avermectin residual have been reported due to the weaker fluorescence signal of a single chromophore[18] or the difficulty in recognizing their complicated chemical structures containing ketones, aldehydes and hydroxyl groups[19]. Therefore, a fluorescent molecule, if rationally designed to contain multiple chromophores and recognition groups, is an ideal probe for monitoring avermectin B_1.

Herein, we report the synthesis of octopus-like 1,3,5-tris (5'-[(*E*)-(*p*-phenoxyazo) diazenyl)] benzene-1,3-dicarboxylic acid) benzene (TPB), with six carboxyl groups and three azo chromophores (Figure. 1). Its application as a fluorescent probe was proved to be feasible by evaluating its fluorescence properties. We further establish a sensitive and specific approach for qualitative and quantitative assay of abamectin B_1 and further evaluated its applicability in apple samples, based on a visible fluorescence signal for this probe towards avermectin B_1 at 420 nm.

Results And Discussion

Fluorescence properties of TPB

The fluorescence property of TPB was investigated, with its precursor 5-(4-hydroxyphenylazo)-isophthalic acid dimethyl ester (DDH) for comparison, which only has one azo chromophores. When TPB and DDH were irradiated by ultraviolet light, TPB displayed a maximum emission at 350 nm and excitation at 290 nm (Figure. 2), while no fluorescence signal was visible for DDH (Figure. 3). The difference of fluorescence property, was attributed to the more released energy of TPB than that of DDH when the excited state electrons returned from the excited singlet state (S) to the spin singlet electron (S_0), which is based on the superposition of fluorescence effect of three azo chromophores. Furthermore, improved fluorescence property of TPB is ascribed to enhance resistance to internal rotation of molecule resulting from the introduction of 1,3,5-tris (bromomethyl) benzene and the expansion of space system effect. Moreover, the Stokes shift of TPB was calculated to be 60 nm. The Stokes shift, is considered to effectively decrease detection errors, resulting from the interference from auto-fluorescent of samples[24] and the spectral overlap between the fluorescent and excitation light[25]. Therefore, we think that TPB was suitable for use as a fluorescent probe.

We further investigated the applicability of TPB to abamectin B_1. Upon the addition of abamectin B_1, the emission band at 350 nm and the excitation band at 290 nm of the probe shifted forward to 420 nm and 360 nm respectively (Figure. 3). Generally, different fluorescence molecules have different excitation and emission spectra, which can determine the specificity and selectivity of analysis by using fluorescent probe. The Stokes shift of 60 nm was calculated and reflected ideal anti-interference ability. This result confirms that abamectin B_1 can be identified by probe TPB under the certain conditions, which indeed underpin qualitative analysis of abamectin B_1.

Furthermore, the fluorescence intensity of the reacted product at 420 nm were examined at different concentrations of abamectin B_1. Figure. 4 shows that the fluorescence intensity of the reacted product at 420 nm were enhanced gradually with the increasing volume of abamectin B_1 (1.0 mg L^{-1}). The which was considered as the basis of quantitative analysis. Therefore, TPB can be used as a fluorescence probe for assessing the level of abamectin B_1.

The mechanism of identifying abamectin B_1 by TPB

To investigate the mechanism of identifying abamectin B_1 by TPB, FT-IR and fluorescence spectroscopy, and ESI-MS were employed to compare the difference of the TPB before and after adding abamectin B_1. After adding abamectin B_1, FT-IR spectrum shows additional peaks at 1645 cm^{-1} and at 1120 cm^{-1} (Figure. S6), corresponding to the ester group. The appearance verifies the recognition of probe TPB to abamectin B_1 that is achieved by esterification. In addtion, a clear red shift of wavelengths was found, which is assigned to the changed conjugate systems of electron-donating and rearranged internal charges prompted by enhanced ability of TPB to capture abamectin B_1. Moreover, ESI-MS spectrum yields a peak at m/z = 2717.1910 (Figure. S7), which corresponds to a new product that is produced between probe TPB and abamectin B_1, thus underlying the mechanism of detection.

The aforementioned identification is attributed to the excellent activity of hydroxyls at C_5 in bamectin B_1[26]. Therefore, a recognition mode was tentatively proposed, i.e., the two carboxyl groups of the probe TPB are used as recognition sites to abamectin B_1 with a molar ratio of 1: 2 (Figure. 5). Thus, octopus-like azobenzene fluorescent probe TPB could sensitively capture the abamectin B_1 using its two carboxyls undergoing esterification. The azobenzene fluorescent probe TPB can sensitively capture the abamectin B_1 using its two carboxyls by undergoing esterification.

Establishment and evaluation of the method

To optimize the determination conditions, effects of different levels of the pH and amount of phosphate buffer were investigated. Figure. S8 shows that the fluorescent intensity of probe TPB at 420 nm was initially increased between pH 5.0 and 6.0, followed by a decrease at pH 6.0-9.0 and eventually by the maximum at pH 6.0. The increase-decrease-maximum trend reflects the proper protonation of carboxyl groups of TPB facilitates the coordination process and enhances the nucleophilicity of hydroxyl of TPB to abamectin B_1. Figure. S9 shows that the fluorescent intensity of probe TPB at 420 nm was initially increased between 0.2 mL and 0.8 mL phosphate buffer (0.2 M, pH 6.0), followed by a stabilization at 0.8-1.2 mL phosphate buffer (0.2 M, pH 6.0). Therefore, the validation of using probe TPB was estimated at 0.8 mL phosphate buffer (0.2 M, pH 6.0), by optimizing the determination conditions, linear equation, correlation coefficients (R^2), limit of detection (LOD), limit of quantification (LOQ) precision and linear range. Apparently, the fluorescent intensity of probe TPB mixed with various concentrations of abamectin B_1 exhibited a good linear relationship at the linear range from 4.4 to 60 μg L^{-1}, giving rise to a LOQ of 4.4 μg L^{-1} (Table S1). In addition, the LOD of the described method was calculated as 1.3 μg L^{-1} (Table S1).

The linear regression equation was thus determined to be Y=3987X − 0.7143 (Figure. 6), where Y is the fluorescent intensity of probe TPB at 420 nm, and X represents the concentration of abamectin B_1. Correlation coefficients (R^2) was determined to be 0.9997, which manifests the satisfactory precision of the method. The enhancement clarifies the suitability of this convenient and sensitive method for determination of the abamectin B_1 with the advantages of tiny LOD, miniature LOQ, excellent precision and epic linear range.

Further comparison was conducted between our fluorescent probe method and those described previously. Table S2 shows that the recovery, linear range and LOQ of our fluorescent probe method are comparable to or exceed those of the other methods reported previously.

A good reproducibility is represent by a relative standard deviation of 2.20 % between eleven parallel experiments shown in Table S1. The final product has an unique fluorescence spectra at EX of 360 nm and EM of 420 nm, which can be considered to embody the specificity and selectivity of the method generally, as mentioned above. Sensitivity of the method is benefit from the six carboxyl recognition sites and three azo response sites of TPB.

Preliminary detection of abamectin B_1 in apple samples

Table 1 shows 2.0 mg mL^{-1}, 3.0 mg mL^{-1} and 1.6 mg mL^{-1} abamectin B_1 in *Malus pumila* mill, Qinguan and Huangxiangjiao, respectively. The recoveries of abamectin B_1 spiked to three apple samples are separately calculated as 98.3%, 101.8% and 104.3% (Table 1), which indicate the suitability of this detection method in apples.

Table 1. Determination of abamectin B_1 concentrations in apple samples and recovery rate of the approach

Sample	Found level (mg mL^{-1})	Added level (mg mL^{-1})	Found level after adding (mg mL^{-1})	Average value (mg mL^{-1})	RSD (%) (n = 3)
Malus	2.0	4.0	6.0	5.93	98.3
pumila mill	2.0	4.0	5.8		
	2.0	4.0	6.0		
Qinguan	3.0	4.0	7.10	7.07	101.8
	3.0	4.0	7.10		
	3.0	4.0	7.00		
Huangxiangjiao	1.6	4.0	5.90	5.77	104.3
	1.6	4.0	5.70		
	1.6	4.0	5.70		

Conclusion

In summary, we have demonstrated the probe TPB synthesized for facile quantitative detection of the residual abamectin B_1 in apples. The octopus-like TPB molecule was characterized using UV-Vis, ^{1}H NMR, FT-IR, ESI-MS and fluorescent spectra. The determination conditions were tuned by varying different pH value and concentration, and a proper condition was achieved at pH 6.0 with LOD and LOQ of 1.3 μg L^{-1} and 4.4 μg L^{-1}, respectively. The mechanism of the probe to identify abamectin B_1 was tentatively proposed in a aromatic nucleophilic substitution through a combined mode of TPB and abamectin B_1 with a molar ratio of 1: 2. In particular, the facile quantitative detection of the residual abamectin B_1 in apples was achieved. Our results show that the novel approach of quantitative assay based on fluorescent probe can be helpful to evaluate the abamectin B_1 in agricultural foods.

Methods

Reagents and materials

Dimethyl 5-aminoisophthalate, 1,3,5-tris (bromomethyl) benzene, phenol, sodium acetate anhydrous, sodium nitrite, sodium hydroxide, *N, N*-dimethylformamide (DMF), ethanol anhydrous, methanol, magnesium sulfate anhydrous, potassium carbonate, sodium chloride, acetonitrile, tetrahydrofuran, hydrochloric acid, sulphuric acid, pH 4.0 phosphate buffer (0.2 M), pH 7.0 phosphate buffer (0.2 M), pH 8.0 phosphate buffer (0.2 M), pH 9.0 phosphate buffer (0.2 M), sodium dihydrogen phosphate anhydrous, sodium phosphate dibasic, potassium bromide, deuterated chloroform, octadecylsilane chemically bonded silica (C_{18}) were purchased from Shanghai Macklin Biochemical Co., Ltd (Shanghai, China) and were of analytical grade. pH 6.0 phosphate buffer (0.2 M) was purchased from Beijing Lanyi chemical products Co., Ltd. (Beijing, China) and were of analytical grade. Quinine sulfate fluorescent standard substance (98.6%) and abamectin B_1 were purchased from Aladdin Biochemical Technology Co., Ltd. (Shanghai, China). Demonized water (18 MΩ cm) was produced by using a water purification system (Water Purification System, Casccada 1, Pall, Beijing, China).

General instrumentation

Fourier-transform infrared spectroscopy (FT-IR) was recorded on a Thermo 330 spectrometer at 500-4000 cm^{-1} wavelengths and a resolution of 3 cm^{-1} over 32 scans. The ultraviolet-visible absorption spectrometry (UV-Vis) was measured with a TECHCOMP UV2600 Spectrometer (TECHCOMP, Shanghai, China) at 200-800 cm^{-1} wavelengths. ^{1}H-nuclear magnetic resonance (NMR) spectrum was recorded on a JNM-ECA 600 MHz-NMR using tetramethylsilane (TMS) (JEOL, Japan). Electrospray ionization mass spectroscopy (ESI-MS) data of TPB and the product were obtained by using a Bruker New ultrafleXtreme MALDI-TOF mass spectrometer at NL: 7,990,000, RT: 4.58-4.66, AV: 34, T: FTMS-*p* ESI and NL: 41,300, RT: 2.13-2.22, AV: 36, T: FTMS-*p* ESI. Fluorescent spectrum was performed using a Hitachi F-7000

spectrometer at Sampling Interval: 5 nm, Scan speed: 12000 nm min^{-1}, EX Slit: 5 nm, EM Slit: 5 nm, PMT Voltage: 700V, Contour interval: 10 nm, Temperature: room temperature.

Preparation of probe TPB

TPB was synthesized by the scheme showed in Figure. S1 based on a previously reported method[20], which was confirmed by FT-IR, UV-Vis, ^1H NMR and ESI-MS. FT-IR: characteristic absorption peaks at 3432 cm^{-1} (C-H of aryl), 1699 cm^{-1} (C=O of carboxyl), 1597 cm^{-1} (N=N), 1499 cm^{-1} (aryl), 1253 cm^{-1} (aryl-N). UV-Vis: λmax 355 nm (azobenzene). ^1H NMR (600 MHz, $CDCl_3$) δ (ppm): 8.71 (s, 3 H), 8.65-8.68 (s, 6 H), 7.94-7.95 (d, 6 H), 7.25 (s, 3 H), 7.0-7.1 (d, 6 H), 5.22 (s, 6 H). HRMS (*m*/*z*, ESI): $[M]^-$ calcd. Found 971.2133 (TPB), 703.1660 (TPB-$C_{14}N_2O_4H_8$), 485.1024 (TPB-$C_{22}N_4O_9H_{22}$). All supplementary data used for confirmation can be found in Figures S2-S5.

General procedure for fluorescent spectra measurement

Tetrahydrofuran, as a solvent, was used to prepare the probe TPB solution (0.06 mmol L^{-1}) and abamectin B_1 solution (1.0 mg L^{-1}). 0.5832 g TPB was added to a volumetric flask and mixed with tetrahydrofuran solution to 10 mL to get probe TPB solution (0.06 mmol L^{-1}). 1.0 mg abamectin B_1 was added to a volumetric flask and mixed with tetrahydrofuran solution to 1 L to get abamectin B_1 solution (1.0 mg L^{-1}).

Fluorescent spectra of probe TPB were analyzed before and after adding abamectin B_1 to ascertain the appropriate excitation wavelength and emission wavelength. One 10 mL colorimetric tube was filled with probe TPB (1.0 mL, 0.06 mmol L^{-1}) and avermectin B_1 (0.2 mL, 1.0 mg L^{-1}). The other was only filled with probe TPB (1.0 mL, 0.06 mmol L^{-1}). Then, they all fixed with tetrahydrofuran to 10 mL. For each sample in colorimetric tubes, test condition of the fluorescence intensity was as follows: Sample mixed time: 10 s, Sampling interval: 5 nm, Scan speed: 12000 nm min^{-1}, EX Slit: 5 nm, EM Slit: 5 nm, PMT Voltage: 700V, Contour interval: 10 nm, Temperature: room temperature, EX WL: 200-600 nm, EM WL: 200-600 nm.

Establishment and validation of the analysis method

To obtain the ideal pH condition of test, considering the emergence of esterification at pH below 5.0 and salt forming at pH above 5.0 for avermectin B_1, the effect of pH 5.0-9.0 on the analysis result was investigated. Five 10 mL colorimetric tubes were filled with probe TPB (1.0 mL, 0.06 mmol L^{-1}) and avermectin B_1 (0.2 mL, 1.0 mg L^{-1}), and fixed to 10 mL with pH 5.0-9.0 phosphate buffer (0.2 M) at room temperature, respectively. For each sample in colorimetric tubes, test condition of the fluorescence intensity was same as that of probe TPB, except EX WL: 360 nm and EM WL: 420 nm. pH 6.0 phosphate buffer (0.2 M) was found as an ideal pH condition and used in following tests.

To obtain the ideal mount of phosphate buffer, the effect of 0.2-1.2 mL phosphate buffer (0.2 M, pH 6.0) was investigated. Six 10 mL colorimetric tubes were filled with probe TPB (1.0 mL, 0.06 mmol L^{-1}) and avermectin B_1 (0.2 mL, 1.0 mg L^{-1}), and fixed with 0.2, 0.4, 0.6, 0.8, 1.0 and 1.2 mL phosphate buffer (0.2 M, pH 6.0) at room temperature, respectively. For each sample in colorimetric tubes, test condition of the fluorescence intensity was same as that of probe TPB, except EX WL: 360 nm and EM WL: 420 nm. 0.8 mL phosphate buffer (0.2 M, pH 6.0) was found as an ideal mount and further applied in followed tests.

To establish the relationship between probe TPB and abamectin B_1, at room temperature, 0.0 mL, 0.1, 0.2, 0.3, 0.4, 0.5 and 0.6 mL abamectin B_1 (1.0 mg L^{-1}) were added to probe TPB (1.0 mL, 0.06 mmol L^{-1}), mixed with 0.8 mL phosphate buffer (0.2 M, pH 6.0) and fixed with tetrahydrofuran to 10 mL, respectively. For each sample, test condition of the fluorescence intensity was same as that of part 2.4, except EX WL: 360 nm, EM WL: 200-700 nm.

To validate the method under analytical control, the limit of detection (LOD), limit of quantification (LOQ), precision and linear range were implemented according to the previous methods[21,22]. A 10 mL colorimetric tubes was mixed with abamectin B_1 (0.20 mL, 1.0 mg L^{-1}) and probe TPB (1.0 mL, 0.06 mmol L^{-1}), mixed with 0.8 mL phosphate buffer (0.2 M, pH 6.0), fixed with tetrahydrofuran to 10 mL and fluorescently detected according to that of probe TPB, except EX WL: 360 nm and EM WL: 420 nm. Eleven groups of parallel experiments were conducted. LOD and LOQ were calculated using the formulas shown in Eq. (1-2). Precision was evaluated using relative standard deviation (RSD). The linear range was from LOQ to the maximum measured value.

$$LOD = 3\,\delta/k \qquad (1)$$

(δ: standard deviation of the experiments, k: slope for the range of the linearity)

$$LOQ = 10\times\delta \qquad (2)$$

(δ: standard deviation of the experiments)

Preparation and analysis of apple samples

Malus pumila mill, Qinguan and Huangxiangjiao were purchased from local Xingfu Supermarket (Beijing, China) and analyzed. Apple samples were prepared according to a published method[23]. Each sample (20.0 g) was respectively added with acetonitrile (10.0 mL) and vigorously shaken for 2.0 min by a vortex mixer. Next, each mixture was mixed with 4.0 g anhydrous magnesium sulfate anhydrous and 1.0 g sodium chloride and shook for another 1.0 min. Following centrifugation at 4000 rpm for 5.0 min, 2.0 mL of the upper layer was transferred to a 20 mL volumetric flask and filled with tetrahydrofuran to obtain tested *Malus pumila* mill, Qinguan and Huangxiangjiao samples. These samples were fluorescently detected according to that of probe TPB, except EX WL: 360 nm and EM WL: 420 nm, respectively. Value of abamectin B_1 was calculated according to the linear regression equation of this work.

To perform the recovery rate, two 10 mL colorimetric tubes were mixed with 2.0 mL apple sample and probe TPB (1.0 mL, 0.06 mmol L^{-1}), mixed with 0.8 mL phosphate buffer (0.2 M, pH 6.0), fixed with tetrahydrofuran to 10 mL and marked as A and B, respectively. Afterwards, A was filled by the standard abamectin B_1 (0.05 mL, 1.0 mg L^{-1}). They all were fluorescently detected according to that of probe TPB, except EX WL: 360 nm and EM WL: 420 nm. Level of abamectin B_1 was calculated according to the linear regression equation of this work. And the recovery rate was calculated using the formulas shown in Eq. (3).

Recovery rate (%) = 100 × (C_A - C_B)/C_S (3)

(C_A: level of abamectin B_1 of A filled by the standard abamectin B_1, C_B: level of abamectin B_1 of B, C_S: level of added standard abamectin B_1)

Declarations

Acknowledgements

This work was supported by the National Natural Science Foundation of China (No. 21671021) and the Fundamental Research Funds for the Central Universities (No. 2015ZCQ-LY-03).

Compliance with ethical standards

Conflicts of interest

The authors declared that there are no conflicts of interest.

Supplementary information

Supplementary data related to this article can be found at Supplementary material.

References

1. Rúbies, A., Antkowiak, S., Granados, M., Companyó, R. & Centrich, Determination of avermectins: A QuEChERS approach to the analysis of food samples. *Food Chem*. **181**, 57-63 (2015).
2. Egerton, J. *et al*. 22, 23-dihydroavermectin B_1, a new broad-spectrum antiparasitic agent. *Br Vet J*. **136**, 88-97 (1980).
3. Shen, H. *et al*. Determination and correlation of Avermectin B_{1a} solubility in different binary solvent mixtures at temperatures from (283.15 to 313.15) K. *J Chem Thermodyn*. **105**, 253-266 (2017).
4. Teixeira, R. , Flores, D. H. Â., da Silva, R. C. S., Dutra, F. V. A. & Borges, K. B. Pipette-tip solid-phase extraction using poly(1-vinylimidazole-co-trimethylolpropane trimethacrylate) as a new molecularly imprinted polymer in the determination of avermectins and milbemycins in fruit juice and water samples. *Food Chem*. **262**, 86-93 (2018).

5. Zhou, Q. *et al*. The effects and mechanism of using ultrasonic dishwasher to remove five pesticides from rape and grape. *Food Chem*. **298**, (2019). https://doi.org/10.1016/j.foodchem.2019.125007
6. Zhan, J. *et al*. Multi-class method for determination of veterinary drug residues and other contaminants in infant formula by ultra performance liquid chromatography-tandem mass spectrometry. *Food Chem*. **138**, 827-834 (2013).
7. Lemos, M. T. *et al*. Development, validation, and application of a method for selected avermectin determination in rural waters using high performance liquid chromatography and fluorescence detection. *Ecotox Environ Safe*. **133**, 424-432 (2016).
8. Zhao, W., Zheng, W. J., He, Y., Wan Y. P. & Wang, S. L. Determination of avermectin residues in animal products by ELISA. *Food Research and Development*. **30**, 39-44 (2009).
9. Park, J. H., Abd El-Aty, A. M., Rahman, M. M., Choi, J. H. & Shim, J. H. Application of hollow-fiber-assisted liquid-phase microextraction to identify avermectins in stream water using MS/MS. *J Sep Sci*. **36**, 2946-2951 (2013).
10. Ni, T. *et al*. Development of a broad-spectrum monoclonal antibody-based indirect competitive enzyme-linked immunosorbent assay for the multi-residue detection of avermectins in edible animal tissues and milk. *Food Chem*. **286**, 234-240 (2019).
11. De Souza Santos Cheibub, A. , Silva Bahiense de Lyra, E. & Pereira Netto, A. D. Development and validation of a method for simultaneous determination of trace levels of five macrocyclic lactones in cheese by HPLC-fluorescence after solid-liquid extraction with low temperature partitioning. *Food Chem*. **272**, 148-156 (2019).
12. Zhao, M. *et al*. Far-red to near-infrared fluorescent probes based on silicon-substituted xanthene dyes for sensing and imaging. *Trac-Trend Anal Chem*. **122**, (2019). https://doi.org/10.1016/j.trac.2019.115704
13. Wu, D. *et al*. Comparative analysis of the interaction of mono-, dis-, and tris-azo food dyes with egg white lysozyme: A combined spectroscopic and computational simulation approach. *Food Chem*. **284**, 180-187 (2019).
14. An, Y. , Tan, H. R. & Zhao, S. Y. Silver carbonate mediated oxidative dehydrogenation of aromatic amines to produce aromatic azo compounds. *Chinese J Org Chem.* **37**, 226-231 (2017).
15. Wu, X. , Wang, P. S., Hou, S. Y., Wu, P. L. & Xue, J. Fluorescence sensor for facile and visual detection of organophosphorus pesticides using AIE fluorogens-SiO_2-MnO_2 sandwich nanocomposites. *Talanta*. **198**, 8-14 (2019).
16. Hussein, B. M., Khairy, G. M. & Kamel, R. M. Fluorescence sensing of phosdrin pesticide by the luminescent Eu(III)- and Tb(III)- bis (coumarin-3-carboxylic acid) probes. *Spectrochim Acta A*. **158**, 34-42 (2016).
17. Kestwal, M., Bagal-Kestwal, D. & Chiang, B. H. Fenugreek hydrogel-agarose composite entrapped gold nanoparticles for acetylcholinesterase based biosensor for carbamates detection. *Anal Chim Acta*. **886**, 143-150 (2015).

18. Wang, J. *et al*. A novel reaction-based fluorescent probe for the detection of cysteine in milk and water samples. *Food Chem*. **262**, 67-71 (2018).
19. Wang, Z., Beier, R. & Shen, J. Immunoassays for the detection of macrocyclic lactones in food matrices-A review. *Trac-Trend Anal Chem*. **92**, 42-61 (2017).
20. Eubank, J. *et al*. On demand: The singular rht net, an ideal blueprint for the construction of a Metal-Organic Framework (MOF) platform. A*ngew Chem Int Edit*. **51**, 10099-10103 (2012).
21. Yan, H. *et al*. A water-soluble fluorescent probe for the detection of thiophenols in water samples and in cells imaging. *Spectrochim Acta A*. **229**, (2019). https://doi.org/10.1016/j.saa.2019.117905
22. Zenaida, G., Olga, M. P., Álvaro, G., José, C. & Belén, A. Quantitative determination of wine polysaccharides by gas chromatography-mass spectrometry (GC-MS) and size exclusion chromatography (SEC). *Food Chem*. **131**, 367-374 (2012).
23. Wilkowska, A. & Biziuk, Determination of pesticide residues in food matrices using the QuEChERS methodology. *Food Chem*. **125**, 803-812 (2011).
24. Yuan, L., Lin, W., Zheng, K., He, L. & Huang, Far-red to near infrared analyte-responsive fluorescent probes based on organic fluorophore platforms for fluorescence imaging. *Chem Soc Rev*. **42**, 622-661 (2013).
25. Ren, T. *et al*. A general method to increase Stokes shift by introducing alternating vibronic structures. *J Am Chem Soc*. **140**, 7716-7722 (2018).
26. Wang, Z. *et al*. Two ultrafast responsive isolongifolanone based fluorescent probes for reversible and sensitive visualization of toxic BF_3 in solution and in gas phase. *Sensor Actuat B-Chem*. **304**, (2019). https://doi.org/10.1016/j.snb.2019.127083

Figures

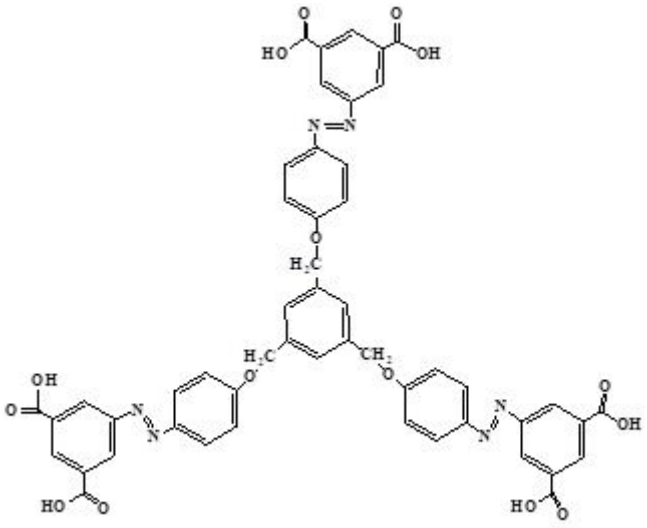

Figure 1

Structure of single molecular TPB

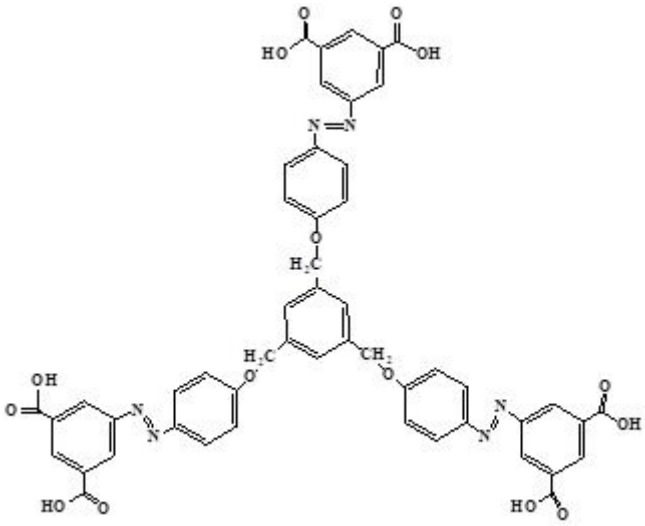

Figure 1

Structure of single molecular TPB

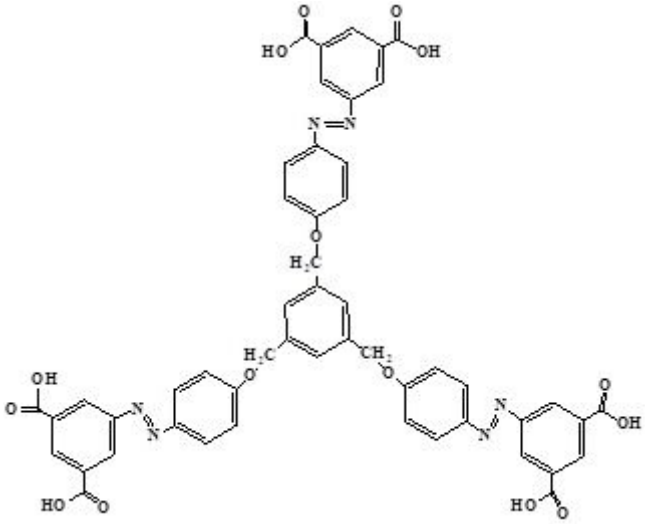

Figure 1

Structure of single molecular TPB

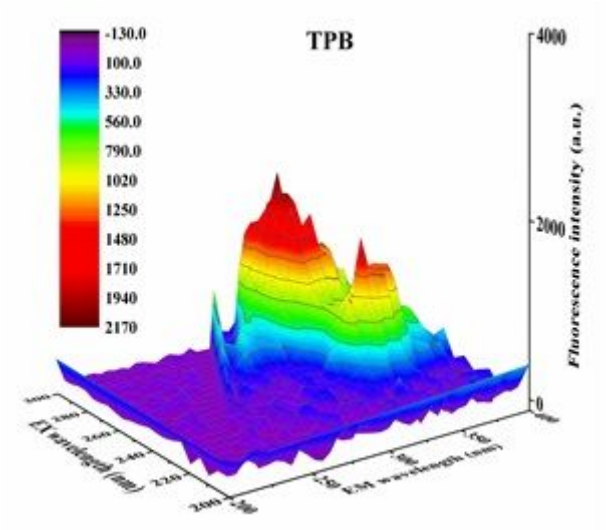

Figure 2

Fluorescence 3D contour spectrum of TPB (0.06 mmol L-1)

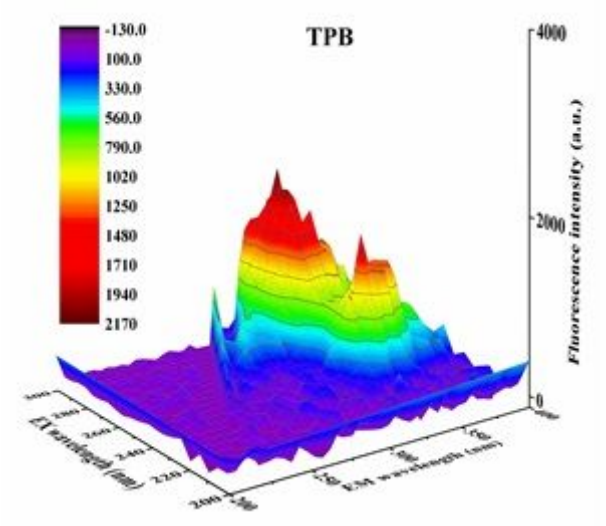

Figure 2

Fluorescence 3D contour spectrum of TPB (0.06 mmol L-1)

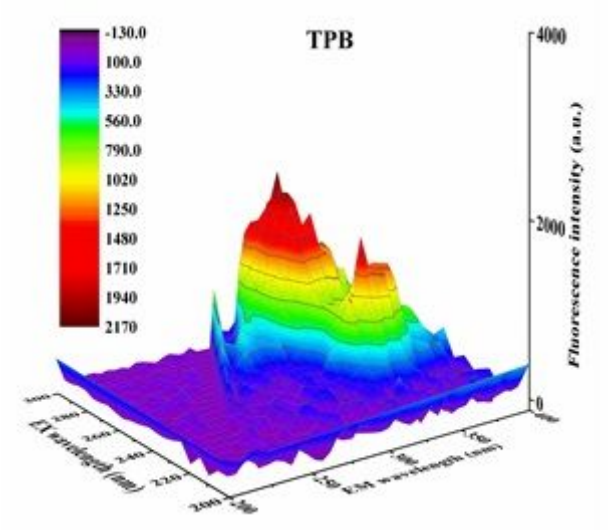

Figure 2

Fluorescence 3D contour spectrum of TPB (0.06 mmol L-1)

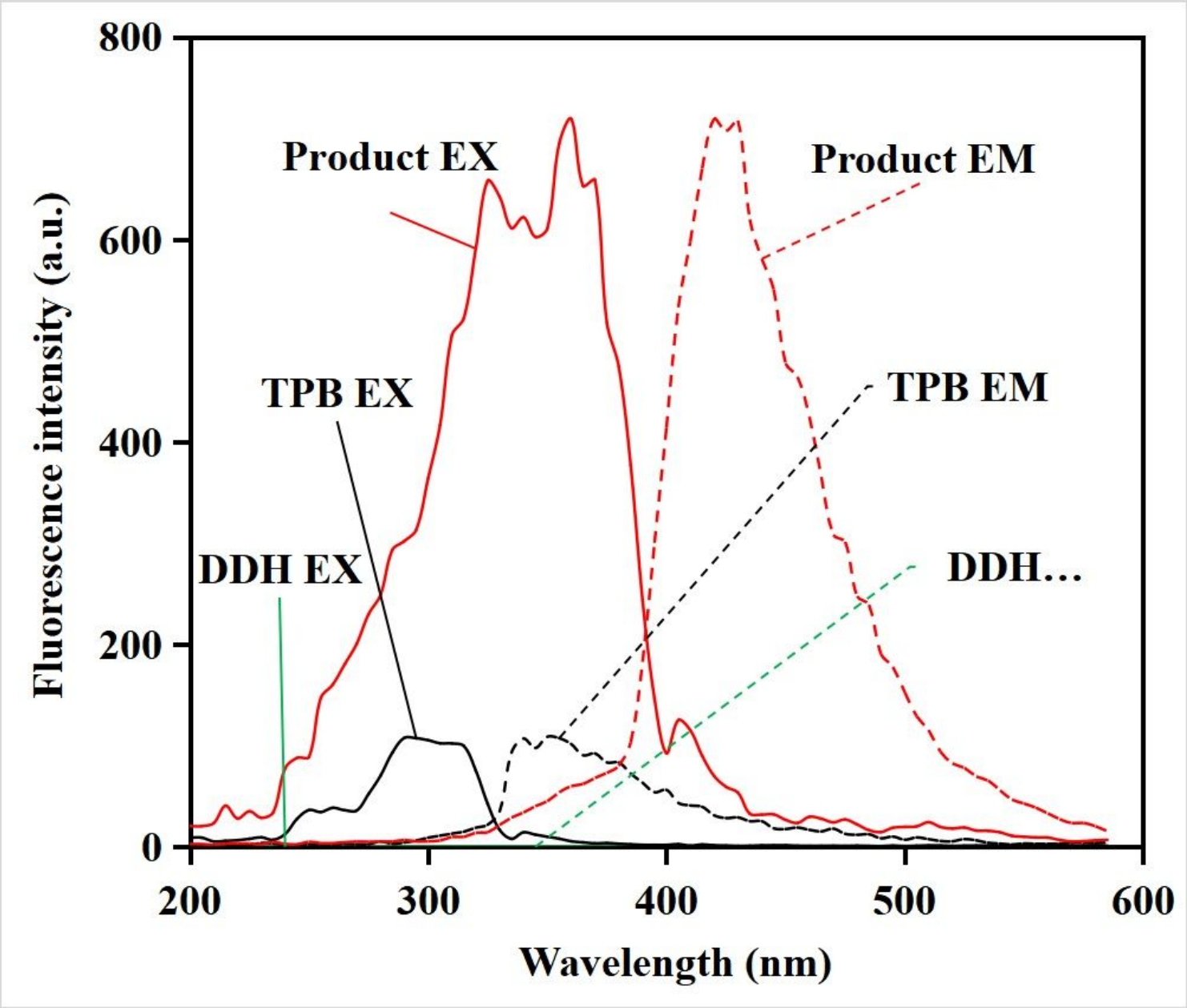

Figure 3

Comparison of fluorescent excitation (EX) and emission (EM) spectra of DDH (0.06 mmol L-1), TPB (0.06 mmol L-1) and the product

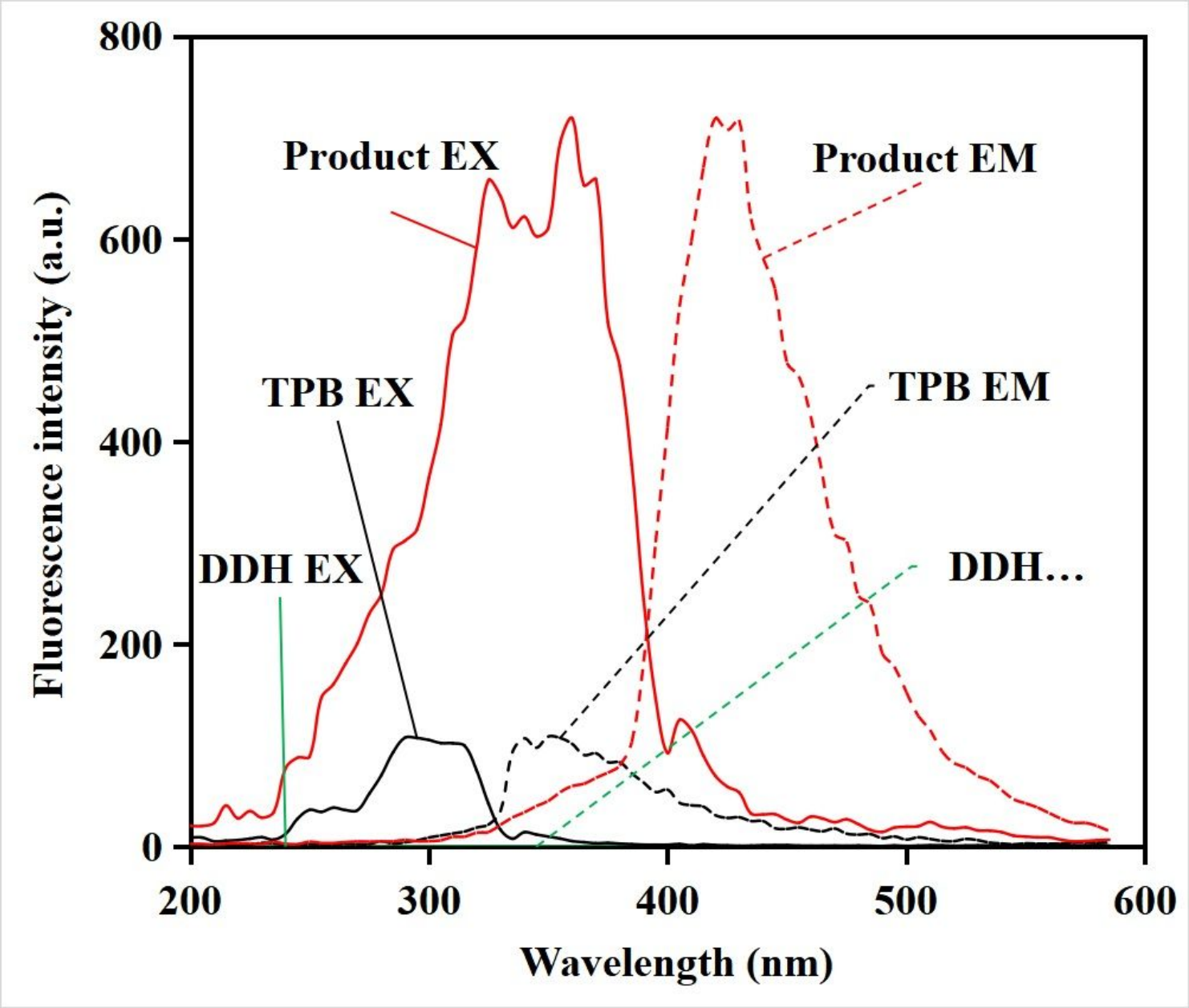

Figure 3

Comparison of fluorescent excitation (EX) and emission (EM) spectra of DDH (0.06 mmol L-1), TPB (0.06 mmol L-1) and the product

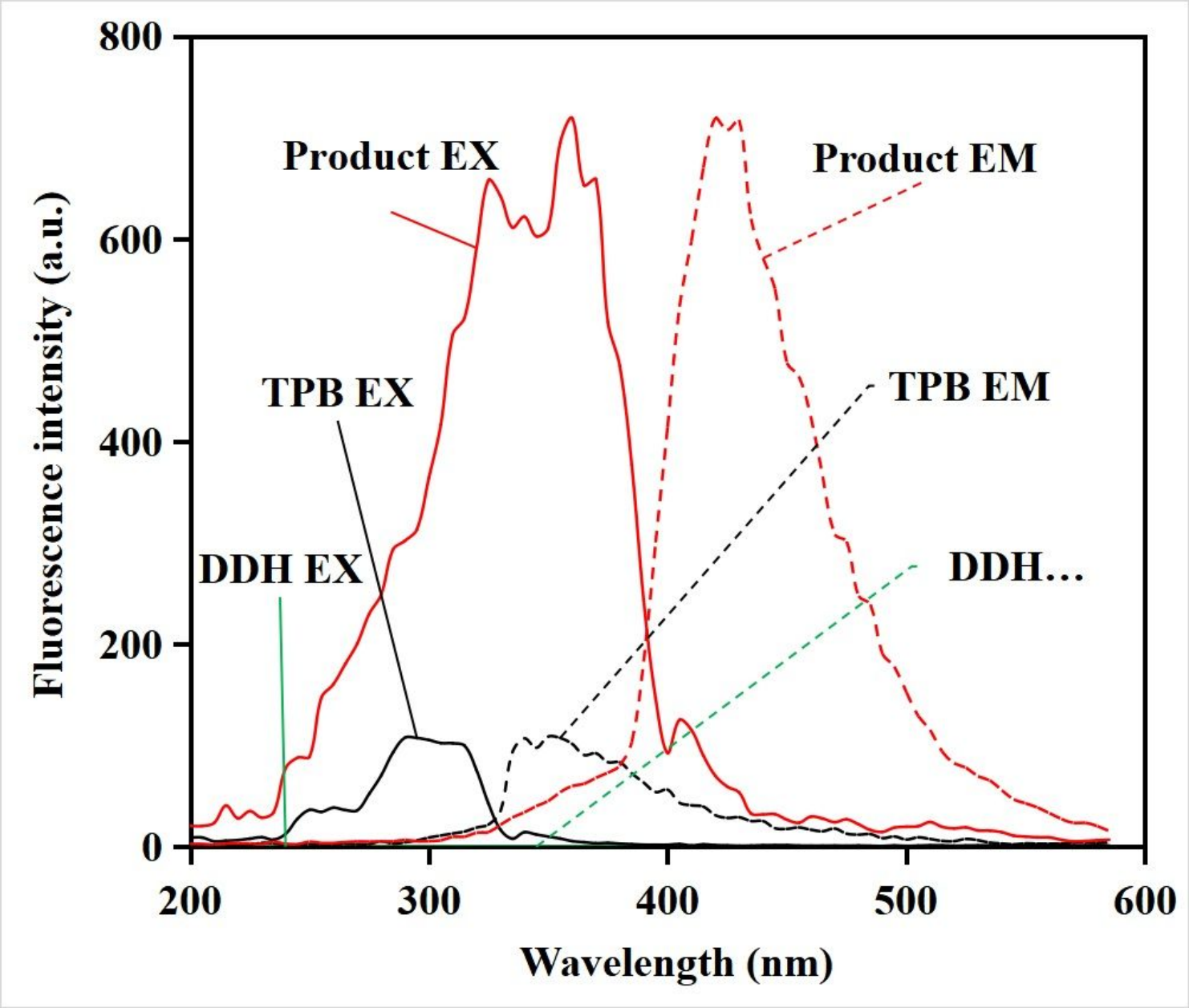

Figure 3

Comparison of fluorescent excitation (EX) and emission (EM) spectra of DDH (0.06 mmol L-1), TPB (0.06 mmol L-1) and the product

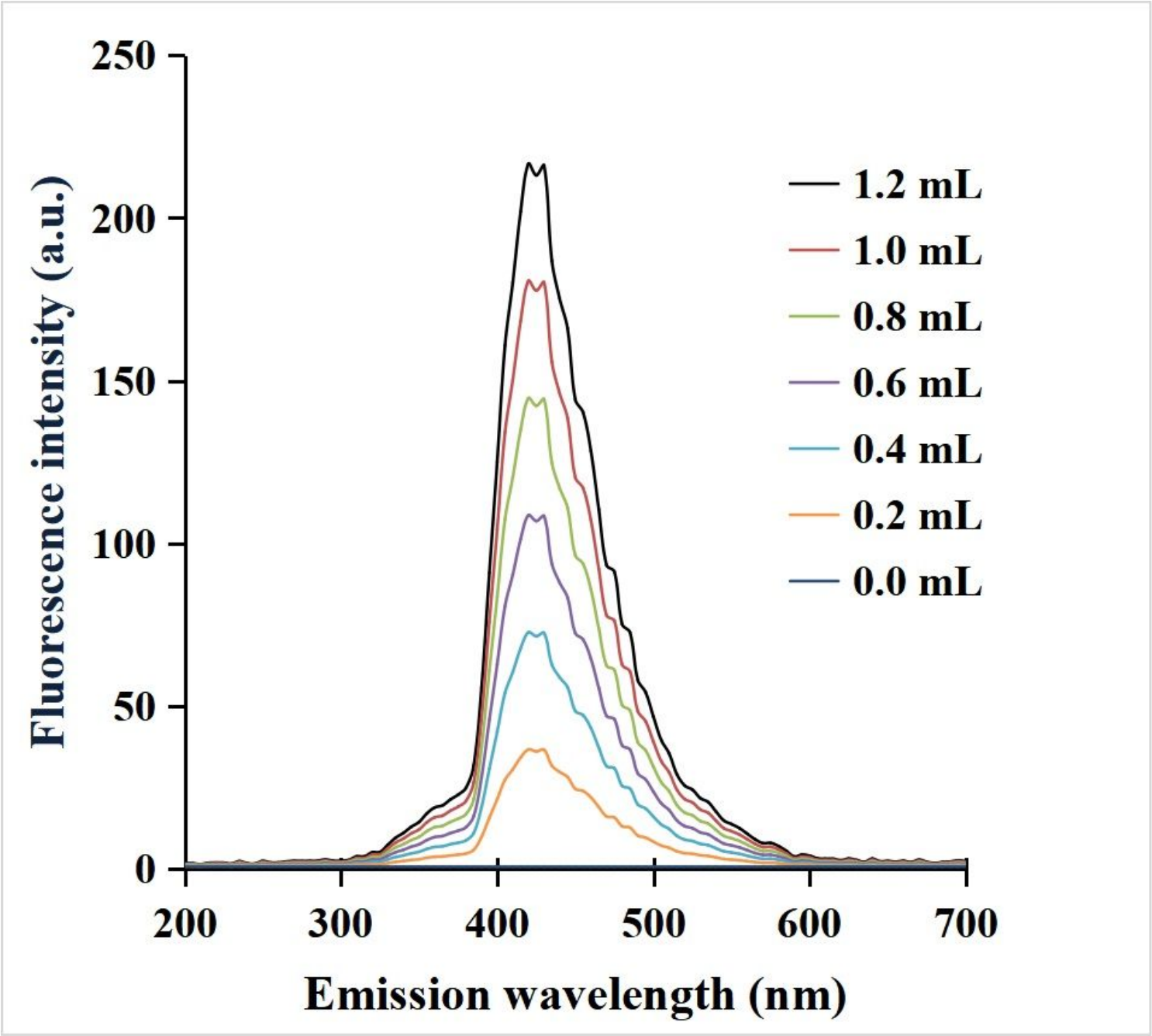

Figure 4

Comparison of fluorescence spectra of the product with 0.0-1.2 mL abamectin B1 (1.0 mg L-1)

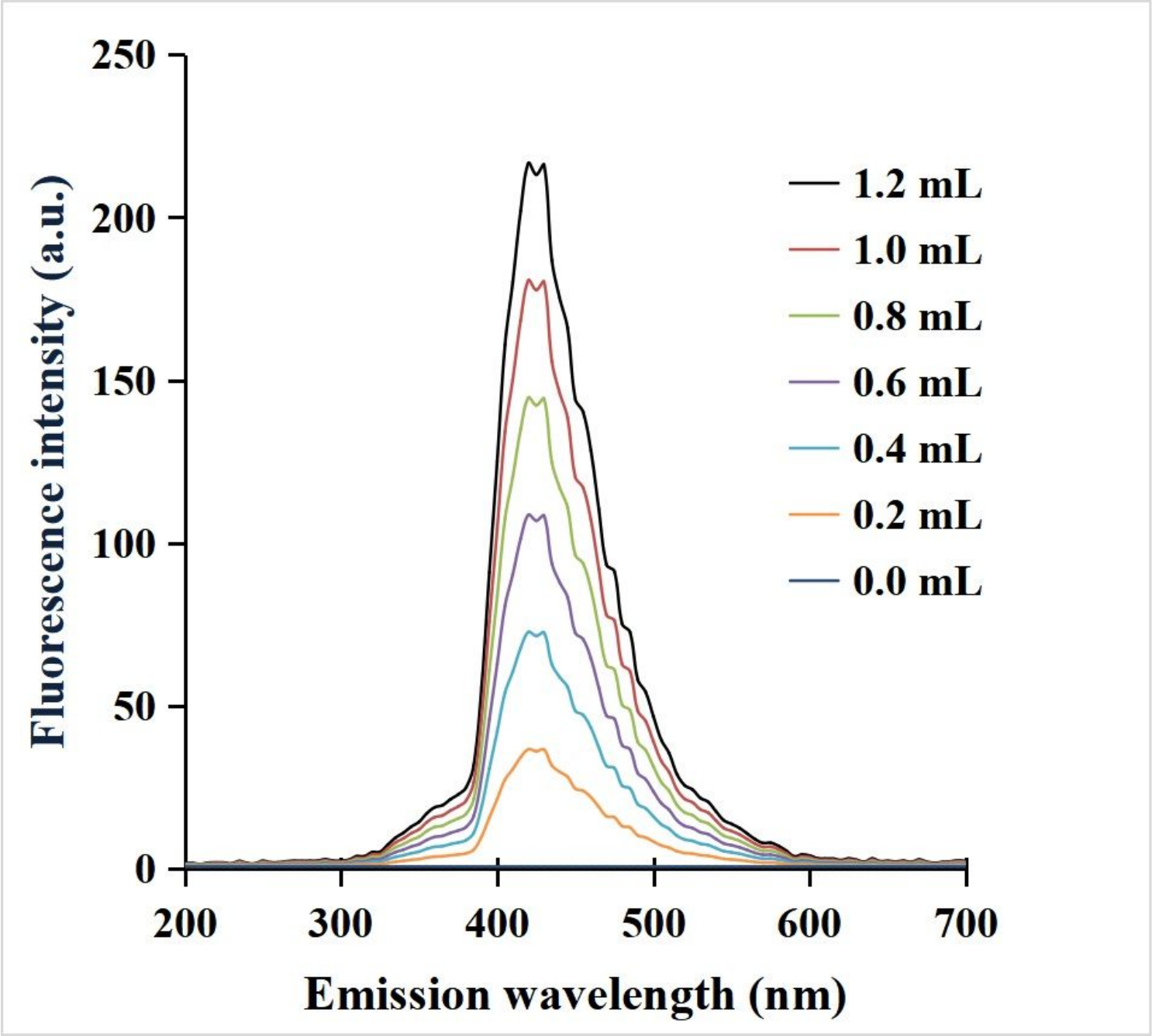

Figure 4

Comparison of fluorescence spectra of the product with 0.0-1.2 mL abamectin B1 (1.0 mg L-1)

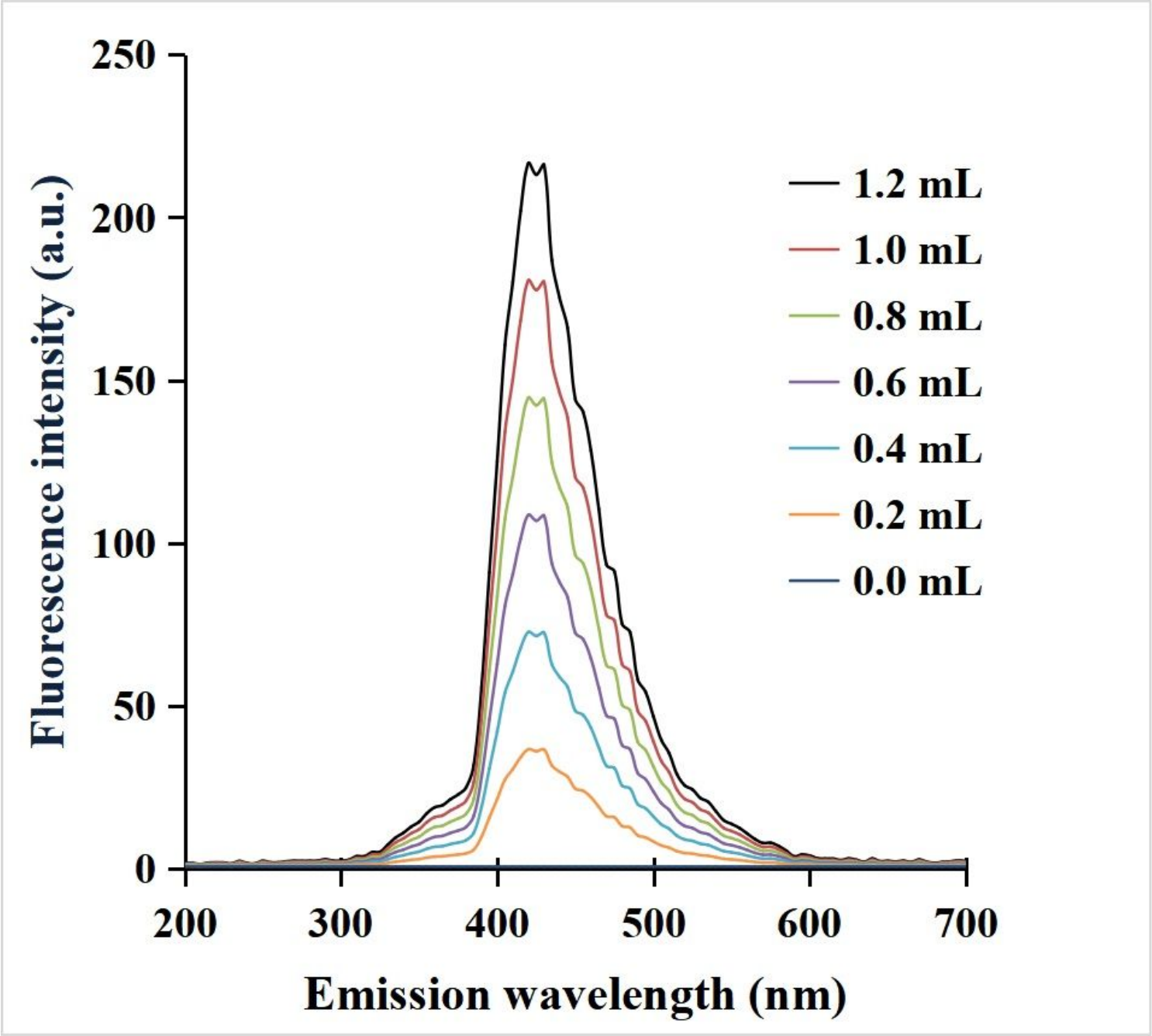

Figure 4

Comparison of fluorescence spectra of the product with 0.0-1.2 mL abamectin B1 (1.0 mg L-1)

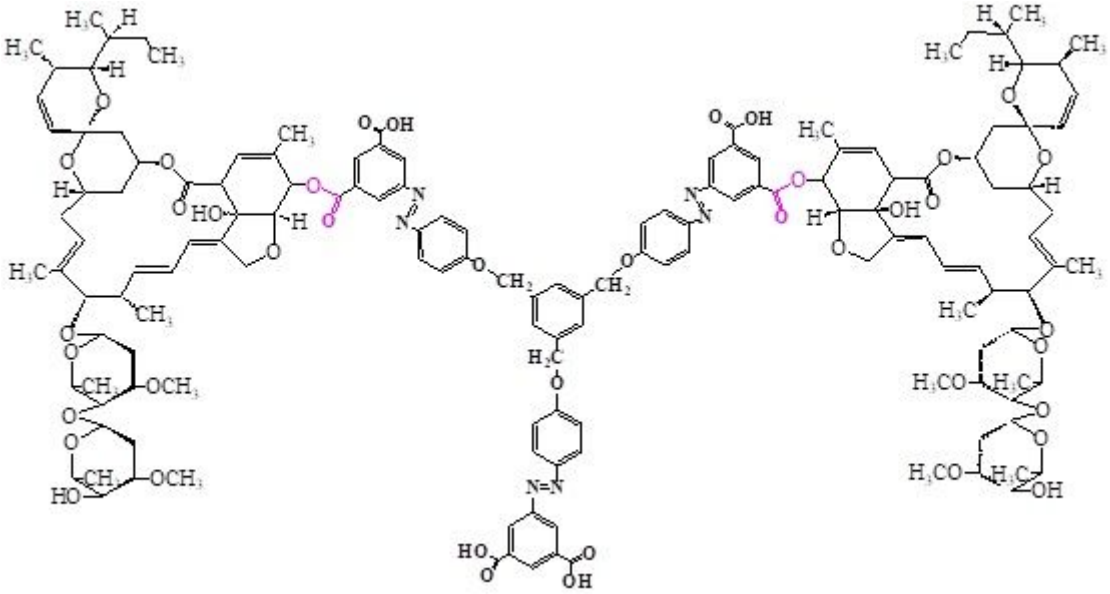

Figure 5

Recognized mode of the reacted product

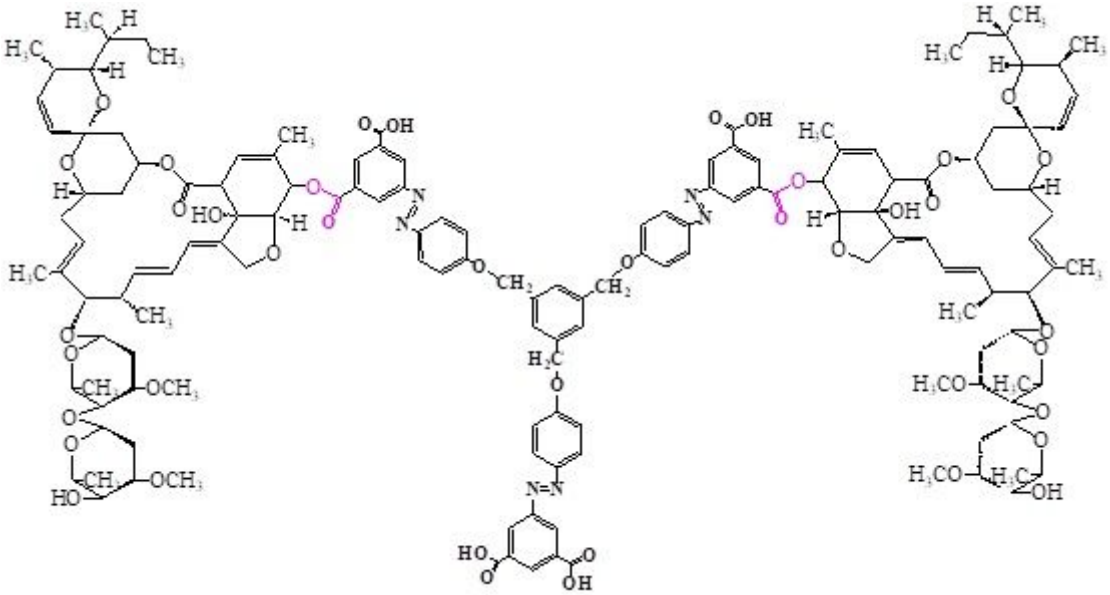

Figure 5

Recognized mode of the reacted product

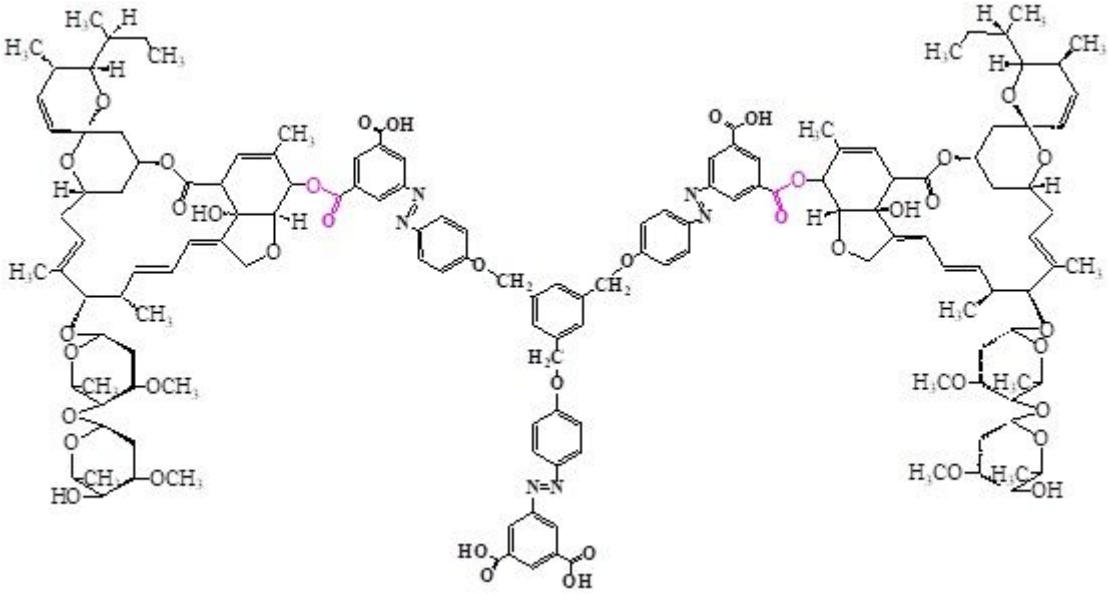

Figure 5

Recognized mode of the reacted product

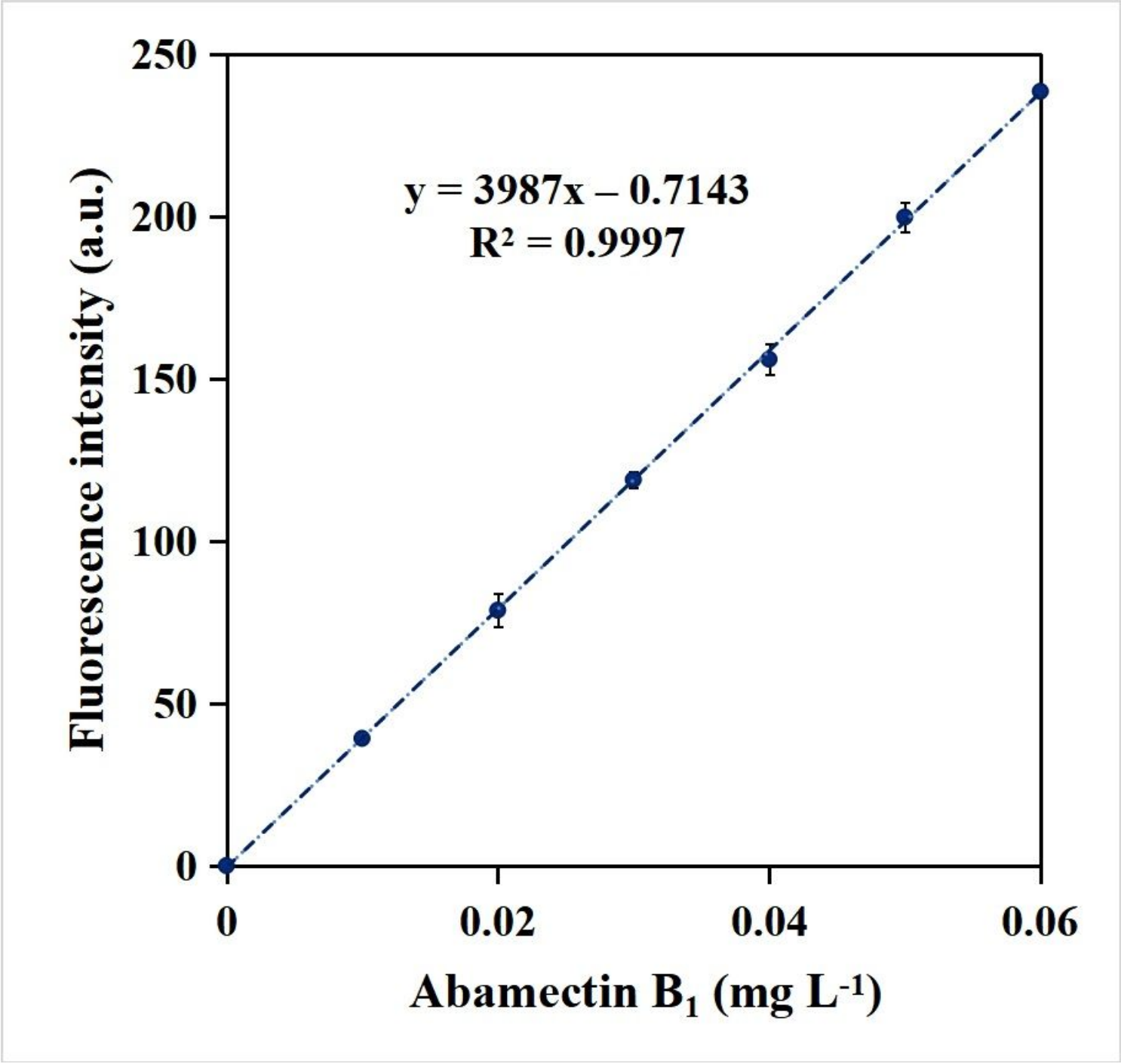

Figure 6

Plot of fluorescence intensity differences with 0.00-0.06 mg L-1 abamectin B1

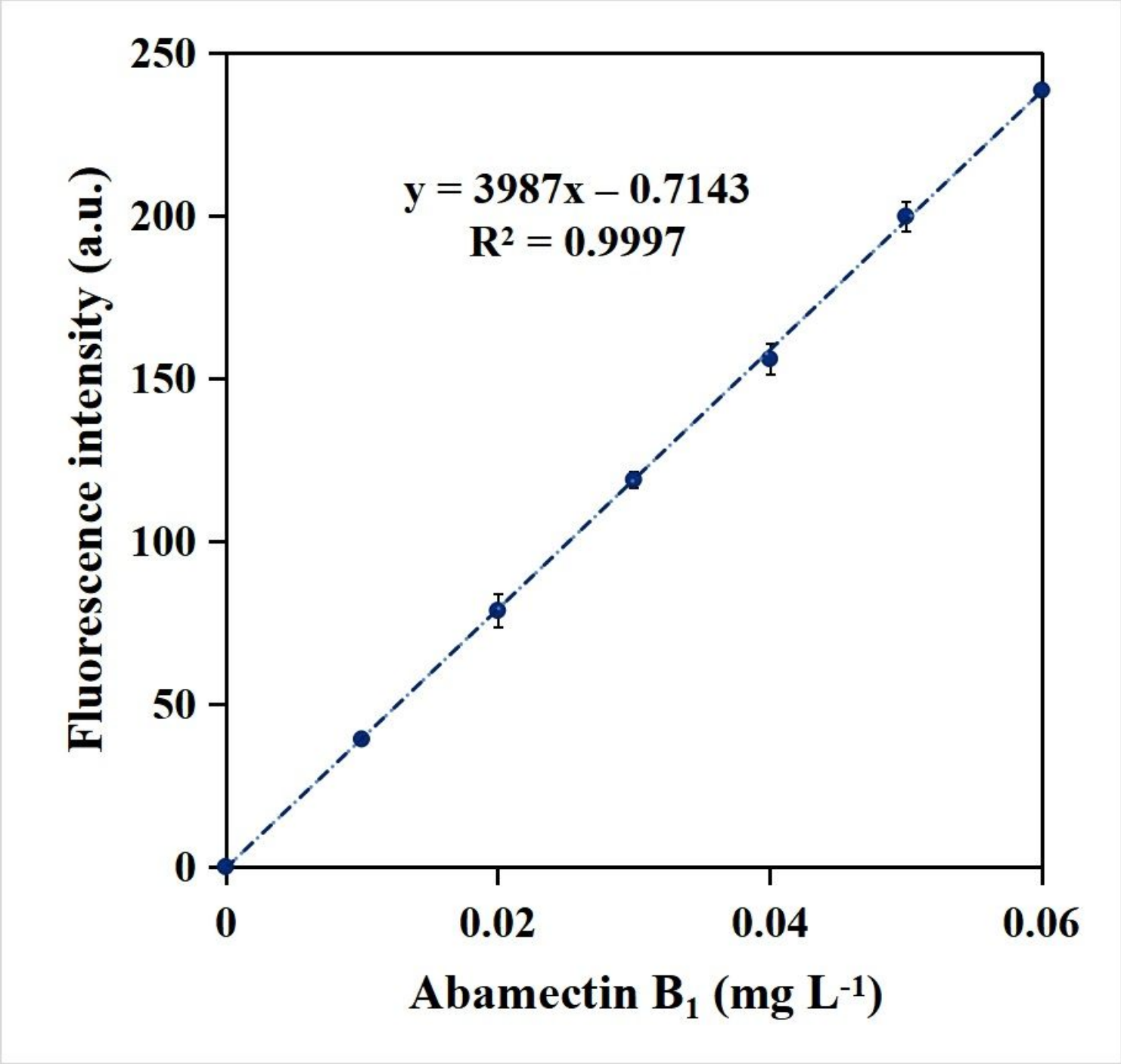

Figure 6

Plot of fluorescence intensity differences with 0.00-0.06 mg L-1 abamectin B1

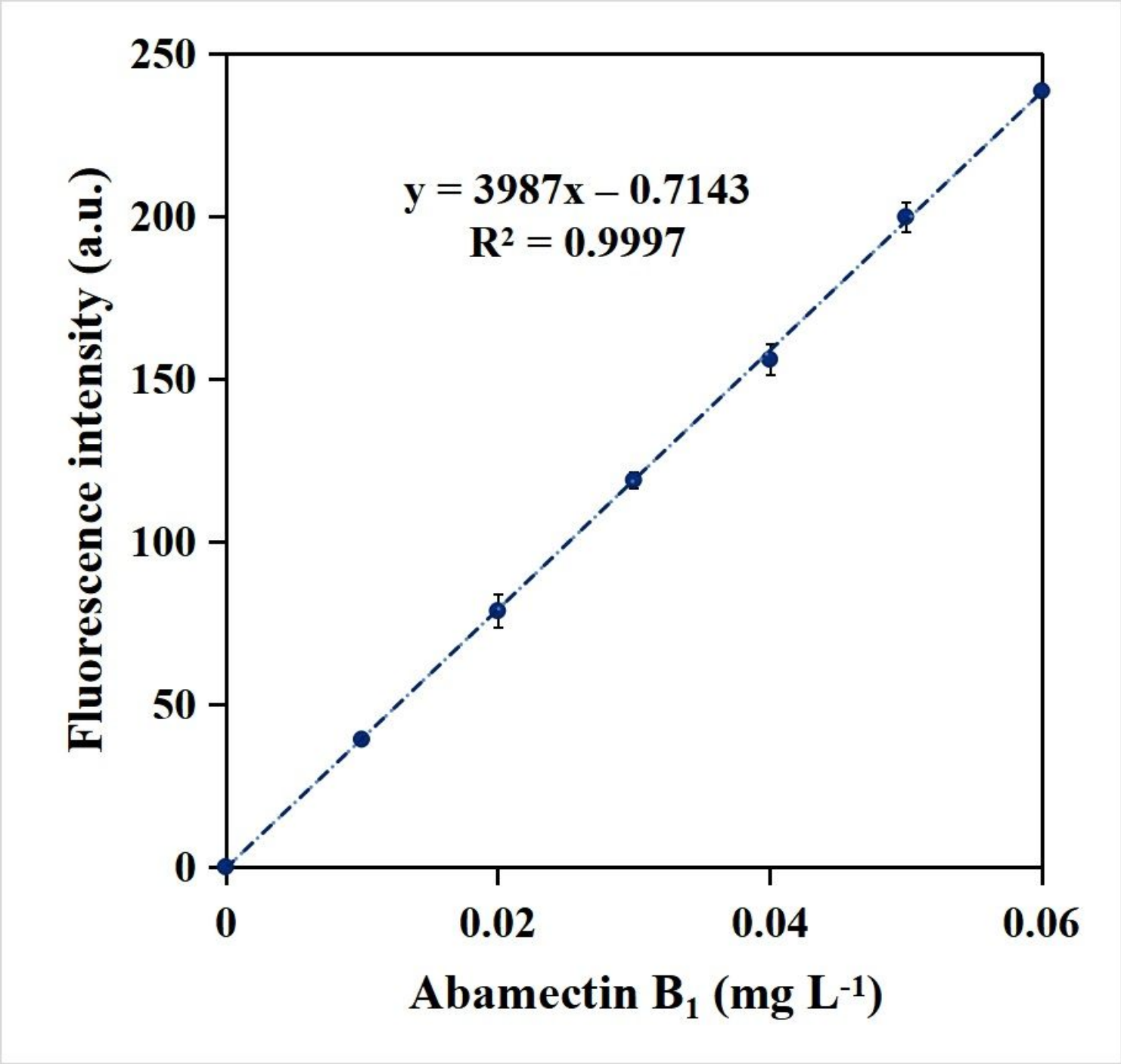

Figure 6

Plot of fluorescence intensity differences with 0.00-0.06 mg L-1 abamectin B1

Supplementary Files

This is a list of supplementary files associated with this preprint. Click to download.

- Supplementarymaterial.doc
- Supplementarymaterial.doc

- Supplementarymaterial.doc